Observation of enhanced Magnetic Transition in *Pbnm* $SmFeO_3$

Jiayu Wang[a], Sameera Ivaturi[a], Shanling Wang[b], Anna Corrias[c] and Filippo S. Boi[a]*

[a] College of Physical Science and Technology Sichuan University, Chengdu China.

[b] Analytical and Testing Centre Sichuan University Chengdu China.

[c] School of Physical Sciences, University of Kent, Canterbury, UK

* corresponding author: f.boi@scu.edu.cn.

Abstract:

Rare-earth orthoferrites $RFeO_3$ materials have recently attracted a great attention for their intriguing technolgical potential. Among these materials, $SmFeO_3$ holds great promise not only for the excellent physical properties (fast magnetic switching, spin reorientation and magnetization reversal) but also for its potential ferroelectric properties which have been recently under debate. Here we focus our attention on T-dependent Zero Field Cooled (ZFC) and Field Cooled (FC) magnetization properties of micrometer scale crystals of $SmFeO_3$ obtained by annealing methods. We report the observation of an enhanced magnetic transition at the temperature of approximately 139 K. From literature bulk susceptibility measurements, is has been suggested that below the temperature of about 140 K, Sm^{3+} moments begin to order antiparallel to the Fe-moments due to antiferromagnetic *f-d* exchange interactions. We attribute the observed transition to compensation effects induced by the appearance of long range ordering in Sm^{3+} spins. The magnetic-nature of the observed transition is confirmed by additional temperature dependent XRD analysis which did not show structural changes of the samples in the same temperature range (from 298 K to 100 K). Due to residual small fractions of ferromagnetic α-Fe from the sample-growth, possible interactions between the magnetic moment of α-Fe and the $SmFeO_3$ crystals at the compensation temperature can not be excluded and could be at the origin of the enhanced magnetic signal reported in this work.

Introduction

Rare-earth orthoferrites $RFeO_3$ (*R*= rare-earth ion) materials have recently attracted a great attention for their intriguing physical properties, ideal for numerous technological applications, such as ultrafast photo-magnetic recording [1-4], inertia-driven spin switching [5], laser-induced ultrafast spin reorientation [6-7], magnetic biasing on *P-E* hysteresis loops [8], enhanced magnetoelectric interactions [9,10], multiferroics, ferroelectrics [11-15]. The family of RMO_3 materials is generally characterized by a distorted perovskite *Pbnm* structure which exhibits a weak ferromagnetic behavior due to a small canting of the antiferromagnetic metal sub-lattices (M^{3+} sub-lattices). In these structures two magnetic sub-lattices can be identified: one due to the 4f-electrons of the rare-earth ions (R-sub-lattice) and another due to the 3d-electrons of the Fe ions (Fe-sub-lattice) [16-21]. One of the most attractive properties of RMO_3 materials is the spin reorientation (SR). SR is a phenomenon which can be induced by temperature and/or by an applied magnetic field. In this type of effect the direction of the easy axis of magnetization has been reported to change from one crystal axis to

another with the change of temperature and/or applied magnetic field parameters [15,16,20,21]. Previous works have attributed the origin of SR to antisymmetric (as described by Dzyaloshinskii [22], Moriya [23], and Treves [24]) and anisotropic-symmetric exchange interactions between Metal (M^{3+}) and Rare-Earth (R^{3+}) magnetic moments [21].

The observed spin configurations and the SR dynamics in RMO_3 are generally classified into 3 configurations, following the Bertaut description, namely Γ_1, Γ_2 and Γ_4 [16]. Among many $RFeO_3$ materials, $SmFeO_3$ has recently attracted a great attention not only for the excellent physical properties such as 1) fast magnetic switching, and 2) easy axis rotation transition (also known as spin reorientation transition) but also for its newly observed room-temperature ferroelectric properties [11-15]. In this type of materials the SR effect involves two main spin configurations, namely Γ_4 at high temperature and Γ_2 at low temperature [15, 16]. These configurations are defined by the symbols Γ_4 (G_x, A_y, F_z) and Γ_2 (F_x C_y, G_z) [21].

In these spin configurations G_x represents the antiferromagnetic spin-configuration of the metal M^{3+} ions along the a-axis and F_z the ferromagnetic spin-configuration along the c-axis. A_y represents the antiferromagnetic-spin-arrangement along the b-axis (due to hidden canting of G_x spins) [21].

The dynamics of the temperature induced SR in this type of material can be explained as follow: as the temperature is lowered, the easy axis of magnetization begins to rotate at a temperature T_2, and ceases to rotate when the rotation angle reaches 90 degrees at another temperature T_1, resulting in spin-configuration Γ_2 (F_x C_y, G_z) where C_y represents another hidden canting spin-configuration [21]. Particularly the dynamics of SR are being recently re-investigated due to possible important correlations of this phenomenon with magnetically driven ferroelectricity effects [11-15].

Recent works have indeed reported the discovery of ferroelectric polarization in $SmFeO_3$ below 670 K (Neel Temperature). The origin of this ferroelectric polarization is highly debated and still not well understood [11-14]. An inverse Dzyaloshinskii-Moriya interaction based mechanism was firstly reported to be the driving force of such ferroelectric properties [11]. However this interpretation was very recently revised due to incompatibilities in the calculated k= 0 magnetic structure, which could not be responsible for the spin-orbit-coupling driven ferroelectric polarization by $S_i \times S_j$ (due to un-broken inversion symmetry) [12]. Thus an alternative mechanism based on $JS_i \cdot S_j$ exchange-striction was then proposed [13]. Such interpretation is still debated and not confirmed by other very recent investigations, where no ferroelectricity has been found in single crystals of the same material ($SmFeO_3$) [14].

In this work we continue to investigate the fascinating physical properties of $SmFeO_3$ materials focusing our attention on T-dependent Zero Field Cooled (ZFC) and Field Cooled (FC) magnetization properties of micrometer scale crystals obtained by annealing methods. Particularly, we report the observation of a not previously reported magnetic transition at the temperature of approximately 139 K. From literature bulk susceptibility measurements, is has been suggested that below the temperature of about 140 K, Sm^{3+} moments would begin to order antiparallel to the Fe-moments due to antiferromagnetic *f-d* exchange interactions. We therefore attribute the observed transition to compensation effects induced by the appearance of long range ordering in Sm^{3+} spins. The magnetic-nature of the observed transition is confirmed by additional temperature dependent Powder X-ray Diffraction analysis which did not show structural changes in the same temperature range (from 298 K to 100 K). Due to residual small fractions of ferromagnetic α-Fe from the sample-growth, possible interactions between the magnetic moment of α-Fe and the $SmFeO_3$ crystals at the compensation temperature can not be excluded. However, no exchange-bias effects

are found in T-dependent hysteresis loops measurements of the produced samples.

Experimental:

The $SmFeO_3$ crystals were prepared by annealing mixtures of Fe-filled carbon foam (produced with the method reported in ref.[26]) and Sm_2O_3 nanoparticles in an Ar and Ar/H_2 flow of 15 ml/min within a chemical vapour deposition system consisting of a quartz tube reactor and an electrical furnace set at the temperature of approximately 990 °C. Transmission electron microscopy (TEM) and Scanning TEM (STEM) investigations were performed by using a 200 kV American FEI Tecnai G^2F20 fitted with field emission gun. Variable temperature XRD analysis was performed with a Panalytical Empyrean powder diffractometer (Cu K-α with λ = 0.154 nm) equipped with a primary Johansson monochromator, an Oxford Cryosystems PhoeniX cryostat, and a X'celerator linear detector. The magnetic measurements (zero field cooled (ZFC), field cooled (FC) and hysteresis loops) were performed by employing a VSM Quantum Design and a VSM Cryogenic Limited London UK.

Results and Discussion

The morphology of the as annealed $SmFeO_3$ crystals was revealed by TEM performed in STEM mode. Due to the high thickness of the crystals, the use of STEM atomic contrast was used for a better visualization of the cross-sectional morphology of the grown crystals. In particular the brighter areas in Fig.1 represent the $SmFeO_3$ phase. Note also the presence of small flakes of grey-like areas which could be associated to residual α-Fe-filled carbon foam not completely oxidized during the annealing process.

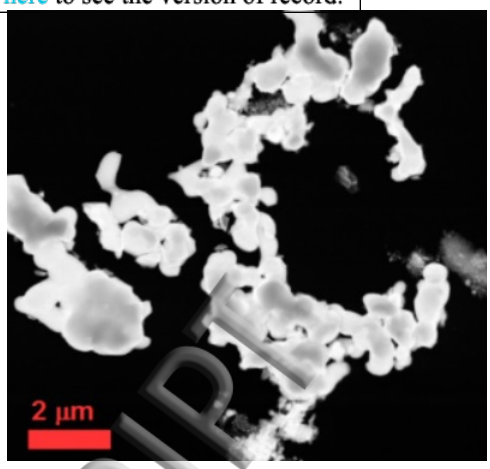

Figure.1: STEM image of a micrometer-scale $SmFeO_3$ crystal flake. The grey areas correspond to the remaining carbon foam flakes not completely oxidized during the annealing process.

The presence of *Pbnm* $SmFeO_3$ crystals within the post-annealed sample was further confirmed by room temperature XRD, as shown in Fig.2. Together with the presence of intense crystalline peaks of $SmFeO_3$, the presence of a residual α-Fe phase was confirmed by the observation of the 110 reflection.

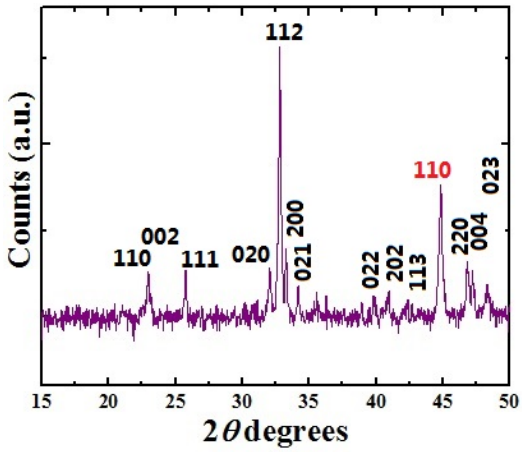

Figure.2: XRD diffractogram of the sample obtained after annealing a mixture of Fe-filled carbon foam and Sm_2O_3 nanoparticles. See Supp. Info. Figs.1-3 for Rietveld Refinement analysis of different portions of the as grown powder sample.

The attention was then turned on the magnetic properties of the produced samples. The presence of a magnetic transition in the temperature range

from 100 K to 200 K was firstly revealed by ZFC measurements as shown in Fig.3.

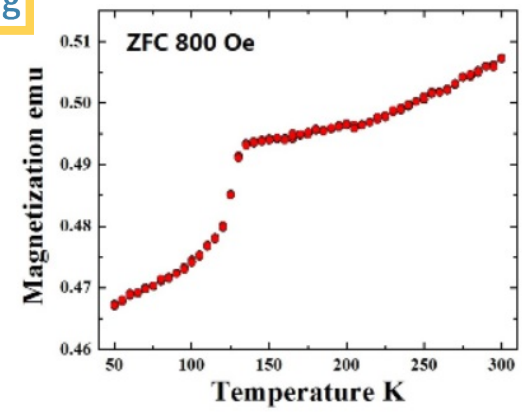

Figure.3: ZFC measurement of the micrometre scale $SmFeO_3$/α-Fe crystals. The used field was 800 Oe.

The existence of such magnetic transition was also confirmed by further FC measurements performed at different fields. Fig.4 shows the typical result of an FC measurement at the applied field of 300 Oe. Furthermore Figs.5-6 show the results of FC measurements at 500 Oe and 800 Oe respectively. It is important to notice that the observed peak is found to become clearer with the increase of the magnetic field used for the FC measurement.

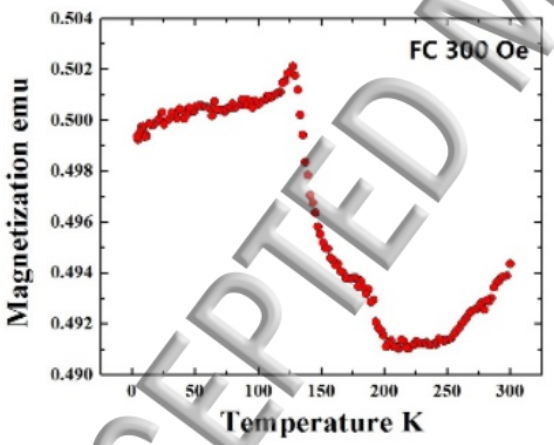

Figure.4: FC measurement of micrometre scale $SmFeO_3$/α-Fe crystals. The used field was 300 Oe.

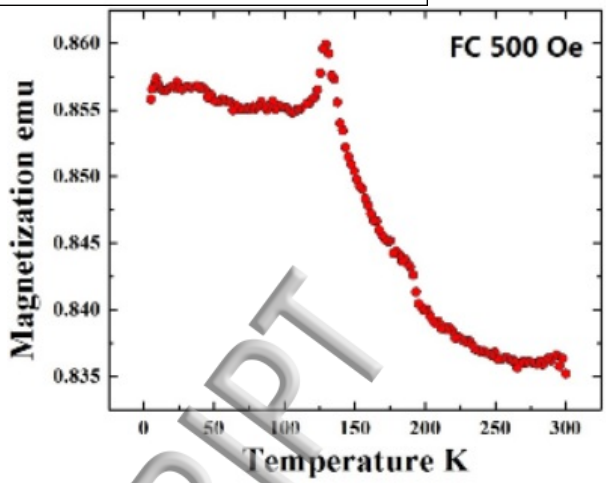

Figure.5: FC measurement of micrometre scale $SmFeO_3$/α-Fe crystals. The used field was 500 Oe.

The observation of this transition cannot be explained on the basis of the previously observed SR phenomenon, which has been generally reported at the temperature in the order of 480 K. Indeed, below the Neel temperature, near 670 K, the weak ferromagnetic moments (associated to the Fe-sublattice spins of the $SmFeO_3$ phase) are expected to re-orient from the c-axis towards the *a*-axis. It has been shown that this effect observed at approximately 480 K causes the *c*-axis susceptibility to decrease rapidly below this temperature, and simultaneously, the *a*-axis susceptibility to rise sharply [25].

Furthermore, the observed transition is not compatible with possible exchange bias effects, since no unusual magnetization or coercivity shifts in the hysteresis loops were found at different temperatures as shown in Fig.7A-B and Fig.8.

Note however that in our samples the hysteresis loops magnetization-dynamics may be influenced by the ferromagnetic behavior of the residual α-Fe component mentioned above (see also Supp. Info.Figs.1-10).

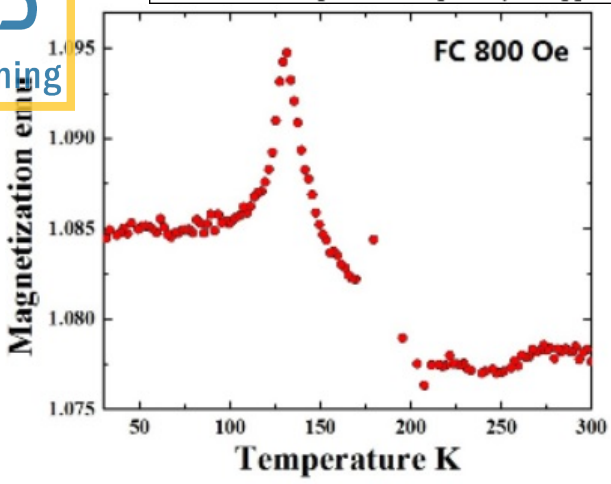

Figure.6: FC measurement of micrometre scale $SmFeO_3$/α-Fe crystals. The used field was 800 Oe.

Instead, considering the low temperature magnetic properties of $SmFeO_3$, an important observation can be made. Indeed at cryogenic temperatures, the magnetization of $SmFeO_3$ has been reported to exhibit a spontaneous magnetization reversal [15,17,18,19,25]. This reversal has been previously attributed to a compensation effect of the weak ferromagnetic moment (associated to the Fe-sublattice spins of the $SmFeO_3$ phase) by antiparallel alignment of the Sm^{3+} moments. Additionally from the bulk susceptibility is has been suggested that below the temperature of about 140 K, Sm^{3+} moments would begin to order antiparallel to the Fe-moments due to antiferromagnetic *f-d* exchange interactions between the two magnetic sub-lattices [25]. Interestingly, recent measurements by Y. K. Jeong et al. [19] revealed a change in the slope of the magnetization curves in their FC measurements from the temperature of approximately 135 K; but no clear magnetization peak was reported. However, it is important to notice that such temperature range is compatible with that observed in our measurements shown in Figs.3-6. Therefore a notable role of the α-Fe ferromagnetic phase on such enhancement of the magnetic transition signal cannot be excluded.

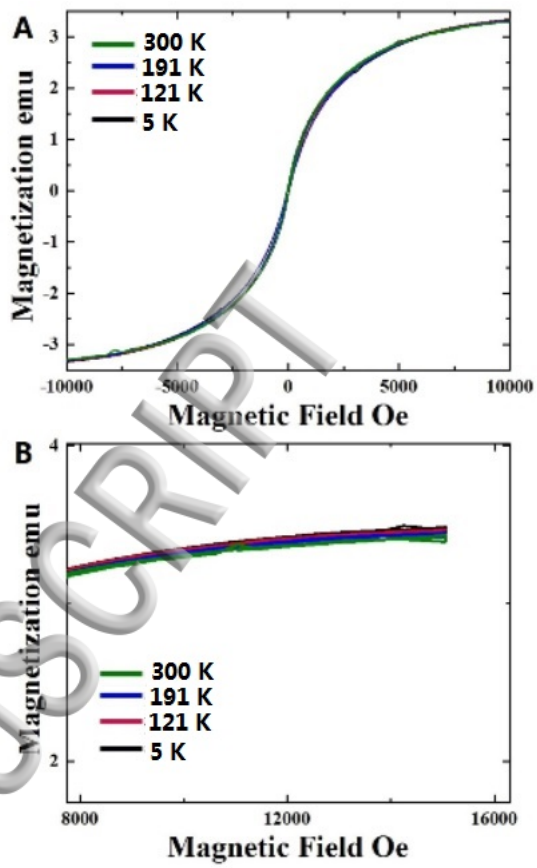

Figure.7: Hysteresis loops of micrometre scale $SmFeO_3$/α-Fe crystals at different temperatures. See Supp. Info. Figs 1-10 for detailed calculations and measurements of the α-Fe contribution to the magnetization.

In the attempt to further confirm the magnetic nature of the observed transition, and therefore exclude possible structural changes within the samples, temperature dependent XRD was carried out. As shown in Figs.9-10 no changes in the structure of the $SmFeO_3$ and α-Fe phases were found in the XRD measurements performed in the temperature range from 298 K to 100 K. These results confirm the interpretations above and suggest that the observed transition in the temperature range between 130 K and 140 K is of magnetic-nature and can be attributed to compensation effects of the ferromagnetic Fe-sublattice moments by antiparallel alignment with the Sm^{3+} moments. This is also confirmed by the fact that Sm^{3+} spins are expected to undergo

long-range ordering from temperatures in the order of 140 K.

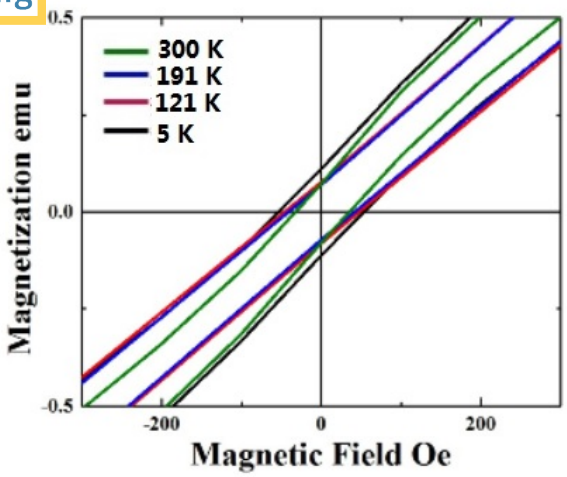

Figure.8: Coercivities parameters from hysteresis loops of micrometre scale $SmFeO_3$/α-Fe crystals at different temperatures.

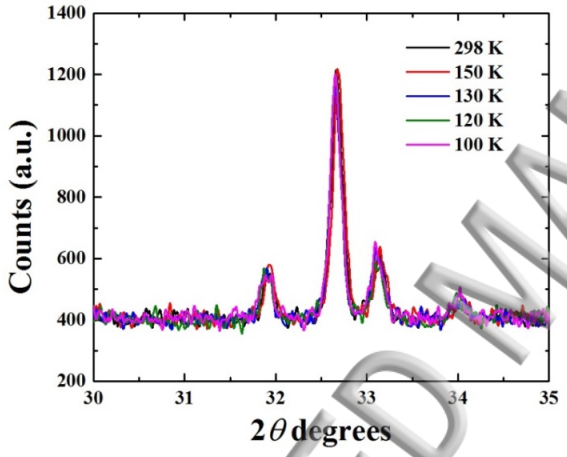

Figure.9: T-dependent XRD measurements in the 2θ range from 30° to 35°.

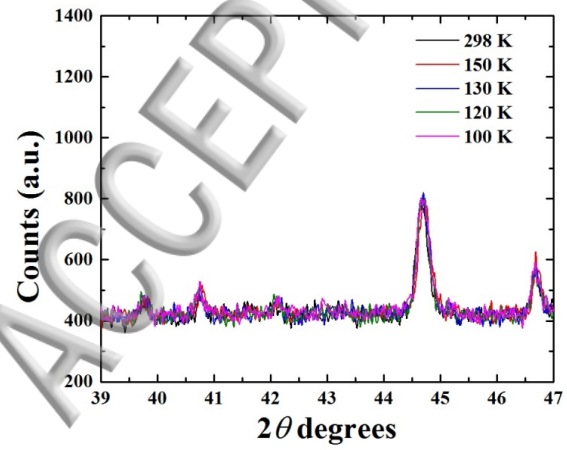

Figure.10: T-dependent XRD measurements in the 2θ range from 39° to 47°.

However future studies will clarify a possible role of the residual α-Fe phase in such magnetic transition and its possible interaction with the Sm^{3+} moments of the $SmFeO_3$ phase.

Conclusion

In conclusion we reported the direct observation of enhanced compensation effects by ZFC and FC measurements of micrometer-scale $SmFeO_3$ crystals obtained by direct high temperature annealing of Fe-filled carbon foam and Sm_2O_3 nanoparticles mixtures in Ar and Ar/H_2 flow. The magnetic nature of the transition was also confirmed by additional temperature dependent XRD which did not show structural changes of the sample in the temperature range from 298 K to 100 K.

Supplementary Material

See supplementary online material for Rietveld Refinement analyses of different portions of the as grown powder sample and detailed calculations and measurements of the α-Fe contribution to the magnetization in the case of 1) the only carbon foam filled with α-Fe (before the annealing stage) and 2) the α-Fe-foam/$SmFeO_3$ crystals reported in this work. Additional SEM images of the $SmFeO_3$ crystals are also shown.

Acknowledgments

We acknowledge Prof. Gong Min and Prof. Hong Zhang for the continuous support. We are also grateful to the National Natural Science Foundation of China grant number 11404227.

References

[1] K. Vahaplar *et al.*, Phys. Rev. B **85**, 104402 (2012).
[2] J. A. de Jong, A. V. Kimel, R. V. Pisarev, A.

Kirilyuk, and T. Rasing, Phys. Rev. B **84**, 104421 (2011).
[3] J. A. de Jong, I. Razdolski, A. M. Kalashnikova, R. V. Pisarev, A. M. Balbashov, A. Kirilyuk, T. Rasing, and A. V. Kimel, Phys. Rev. Lett. **108**, 157601 (2012).
[4] A. V. Kimel, C. D. Stanciu, P. A. Usachev, R. V. Pisarev, V. N. Gridnev, A. Kirilyuk, and T. Rasing, Phys. Rev. B **74**, 060403 (2006).
[5] A. V. Kimel, B. A. Ivanov, R. V. Pisarev, P. A. Usachev, A. Kirilyuk, and T. Rasing, Nat. Phys. **5**, 727 (2009).
[6] A. V. Kimel, A. Kirilyuk, A. Tsvetkov, R. V. Pisarev, and T. Rasing, Nature (London) **429**, 850 (2004).
[7] L. Le Guyader, A. Kleibert, F. Nolting, L. Joly, P. M. Derlet, R. V. Pisarev, A. Kirilyuk, T. Rasing, and A. V. Kimel, Phys. Rev. B **87**, 054437 (2013).
[8] Y. Tokunaga, Y. Taguchi, T. Arima, and Y. Tokura, Phys. Rev. Lett. **112**, 037203 (2014).
[9] T. Kimura, T. Goto, H. Shintani, K. Ishizaka, T. Arima, and Y. Tokura, Nature (London) 426, 55 (2003).
[10] S.-W. Cheong and M. Mostovoy, Nat. Mater. 6, 13 (2007).
[11] J.-H. Lee, Y. K. Jeong, J. H. Park, M.-A. Oak, H. M. Jang, J. Y. Son, and J. F. Scott, Phys. Rev. Lett. 107, 117201 (2011).
[12] R. D. Johnson, N. Terada, and P. G. Radaelli, Phys. Rev. Lett. 108, 219701 (2012).
[13] J.-H. Lee, Y. K. Jeong, J. H. Park, M.-A. Oak, H. M. Jang J. Y. Son, and J. F. Scott, Phys. Rev. Lett. 108, 219702 (2012).
[14] C.-Y. Kuo, Y. Drees, M. T. Fernández-Díaz, L. Zhao, L. Vasylechko, D. Sheptyakov, A. M. T. Bell, T.W. Pi, H.-J. Lin, M.-K. Wu, E. Pellegrin, S. M. Valvidares, Z.W. Li, P. Adler, A. Todorova, R. Küchler, A. Steppke, L. H. Tjeng, Z. Hu, and A. C. Komarek. Phys. Rev. Lett. 113, 217203 (2014)
[15] S. Cao, H. Zhao, B. Kang, J. Zhang and W. Ren. Scientific Reports 4, 5960 (2014).
[16] R. L. White, J. Appl. Phys. 40, 3 (1969).
[17] H. Z. Zhao, et al. J. Appl. Phys. 114, 113907 (2013).
[18] L. G. Marshall, et al. Phys. Rev. B 86, 064417 (2012).
[19] Y. K. Jeong, J. H. Lee, S. J. Ahn, and H. M. Jang. Solid State Commun. 152, 1112 (2012).
[20] R.M.White and R.L.White. Phys.Rev.Lett. **20**, 62 (1968)
[21] T.Yamaguchi. J. Phys. Chem. Solids.. 35,. 479 (1974)
[22] I. Dzyaloshinski, J. Phys. Chem. Solids **4**, 241 (1958).
[23] T. Moriya, Phys. Rev. **120**, 91 (1960).
[24] D. Treves, Phys. Rev. **125**, 1843 (1962).
[25] S. Chaturvedi, P. Shyam, R.Bag，M. M. Shirolkar, J. Kumar, H. Kaur, S. Singh, A.M. Awasthi, and S. Kulkarni. Phys. Rev. B. **96**，024434 (2017).
[26] F.S.Boi et al. Carbon, **101**, 28-36 (2016).

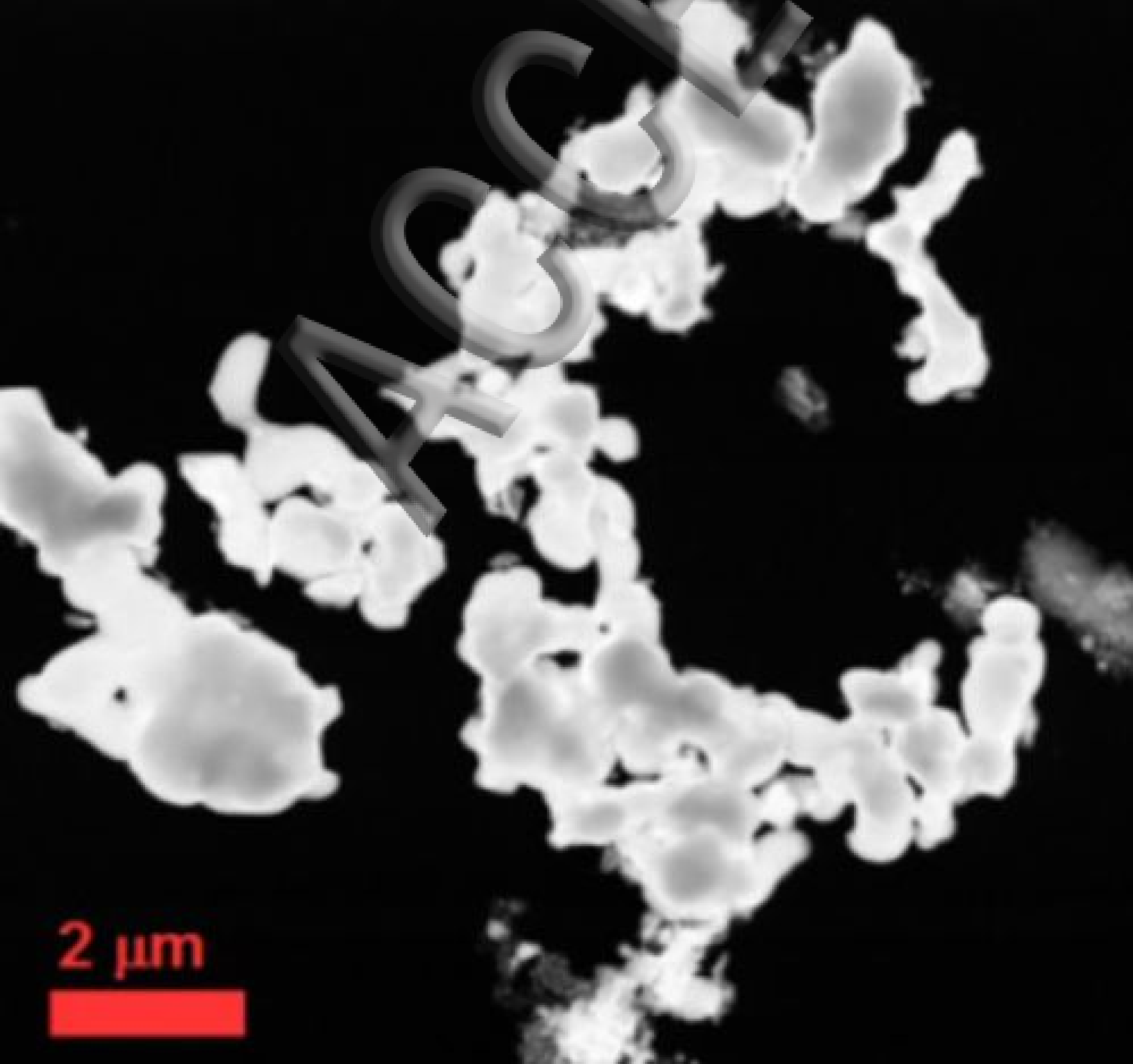
2 µm

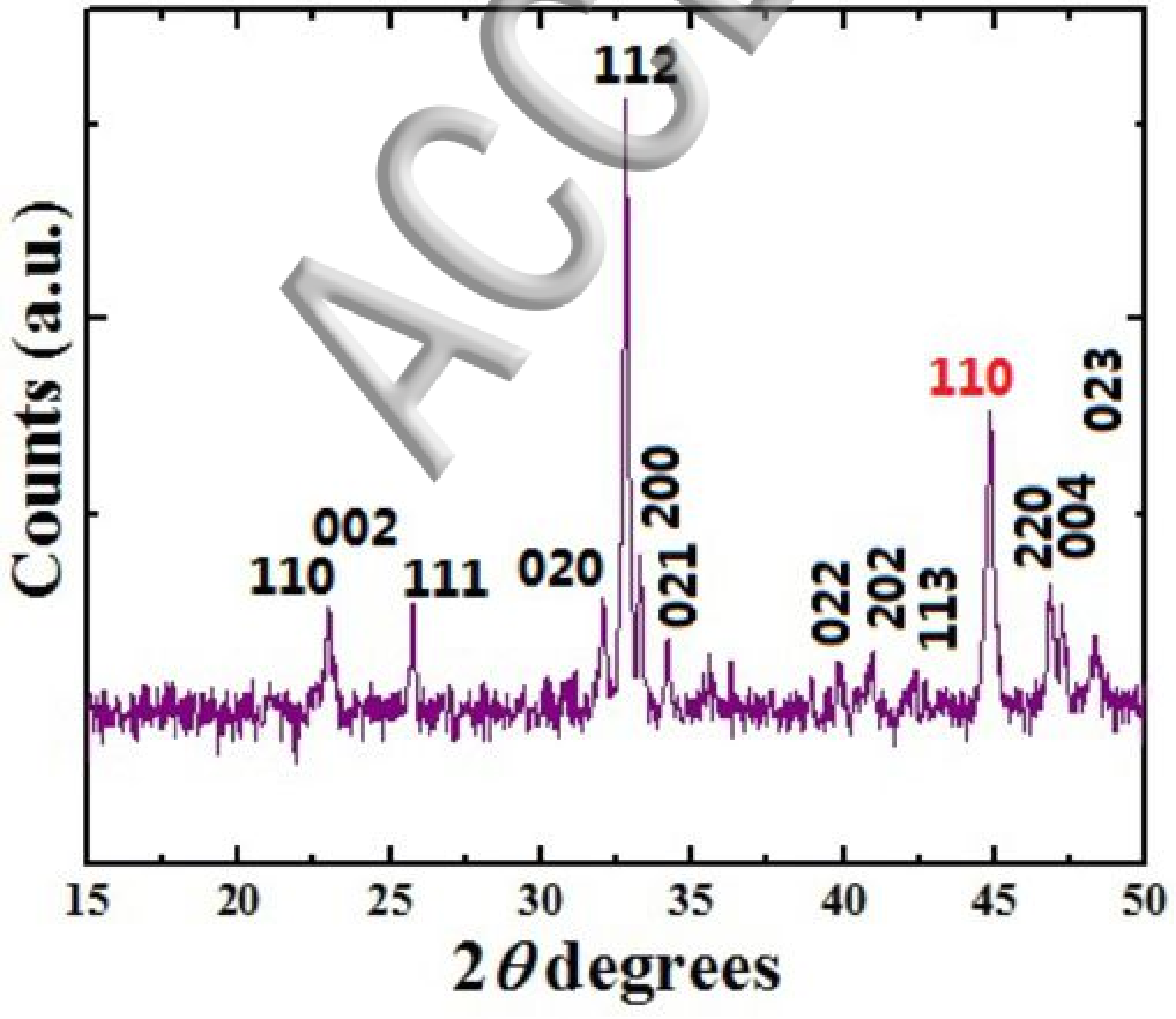
112
110
002
110
111
020
200
021
022
202
113
220
004
023
Counts (a.u.)
15
20
25
30
35
40
45
50
2θ degrees

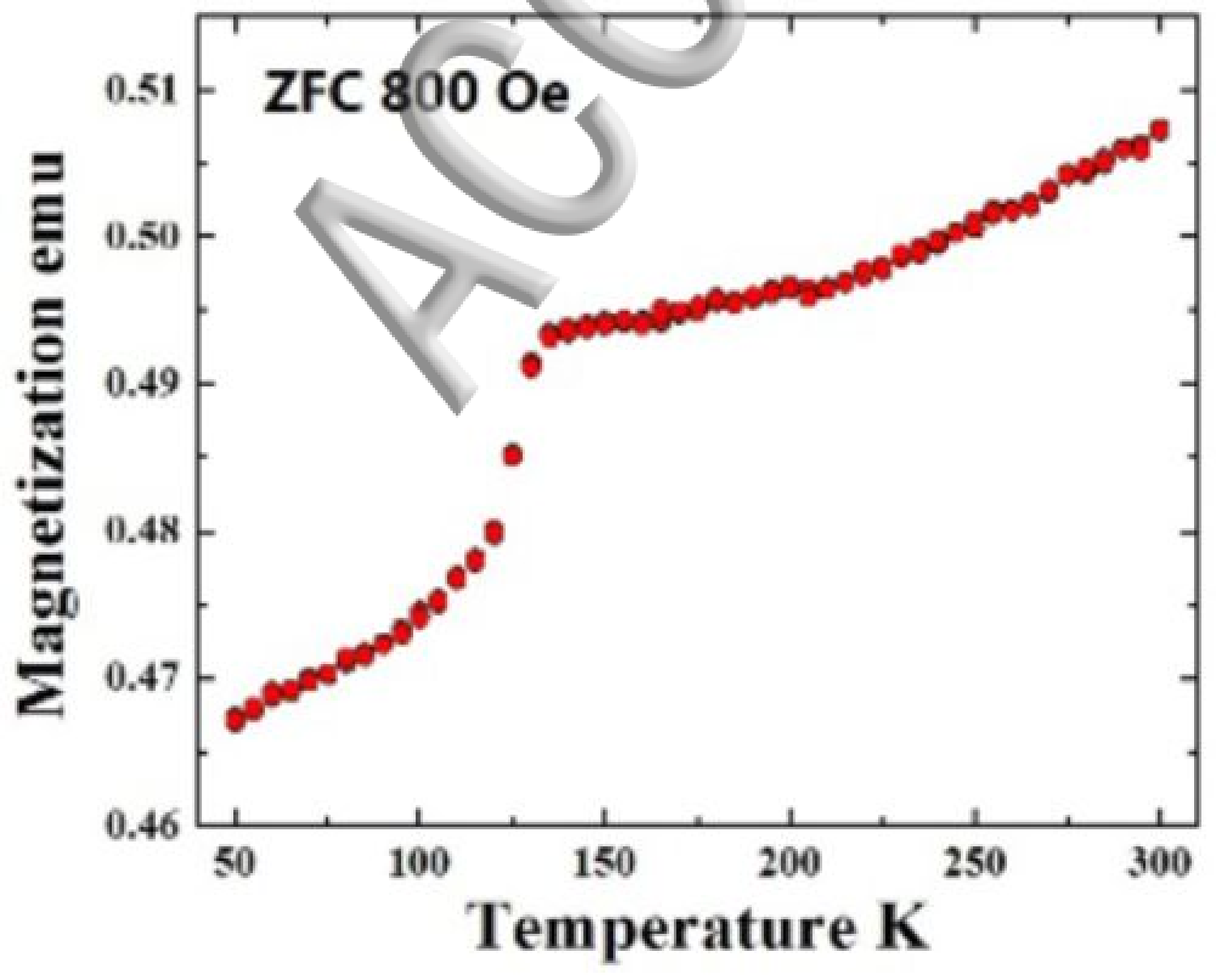
ZFC 800 Oe
Magnetization emu
0.51
0.50
0.49
0.48
0.47
0.46
50
100
150
200
250
300
Temperature K

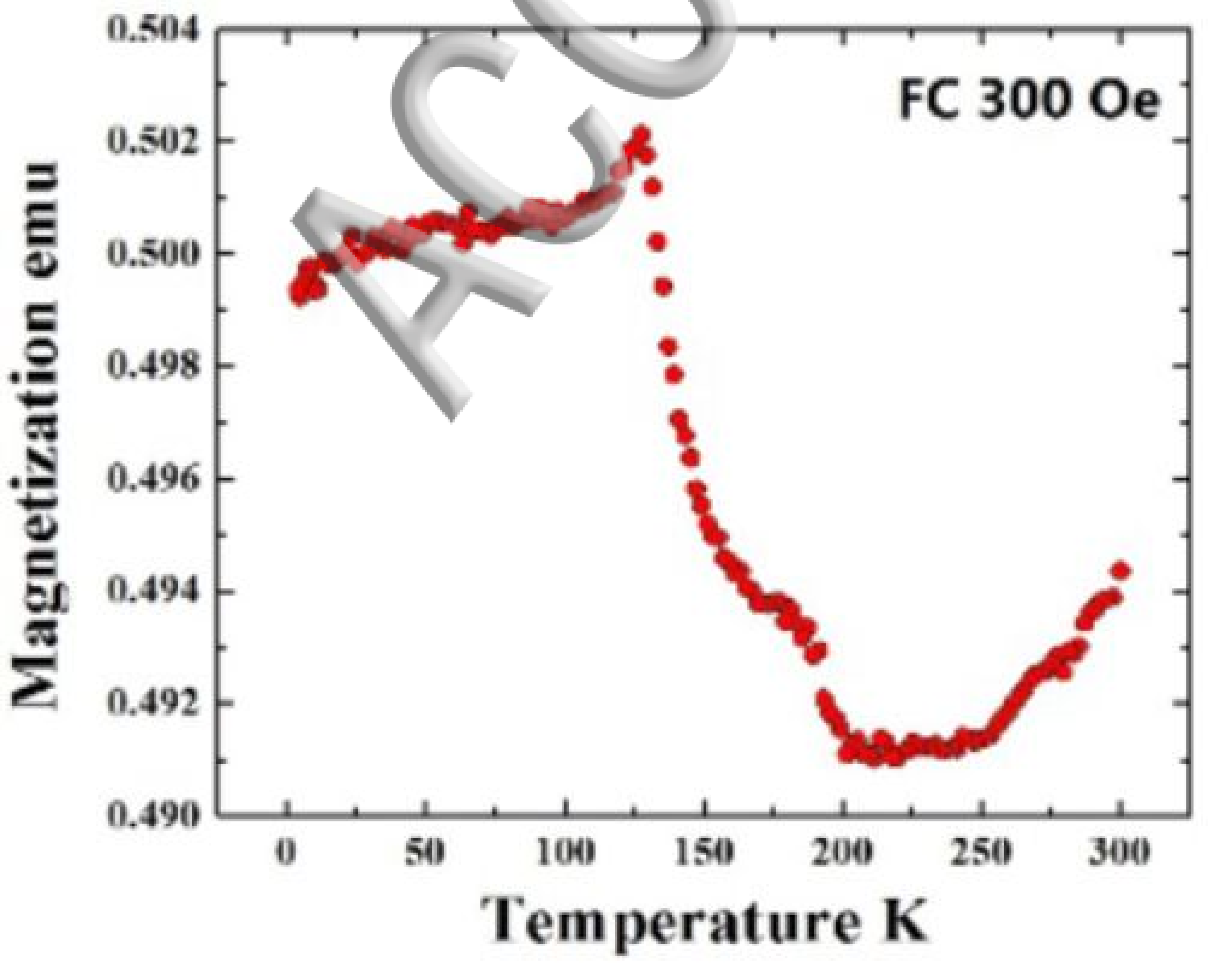
FC 300 Oe
Magnetization emu
0.504
0.502
0.500
0.498
0.496
0.494
0.492
0.490
0
50
100
150
200
250
300
Temperature K

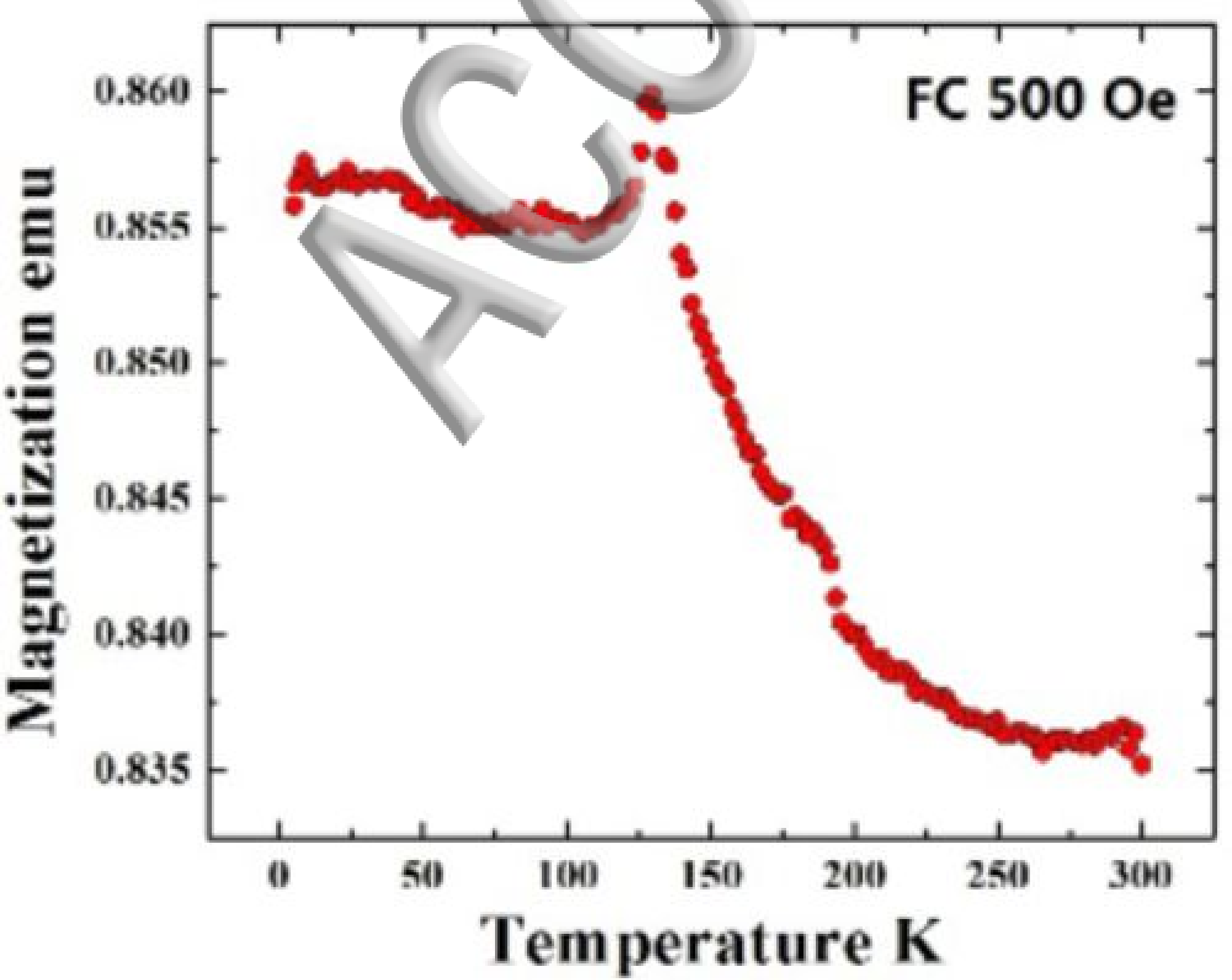
FC 500 Oe
Magnetization emu
0.860
0.855
0.850
0.845
0.840
0.835
0
50
100
150
200
250
300
Temperature K

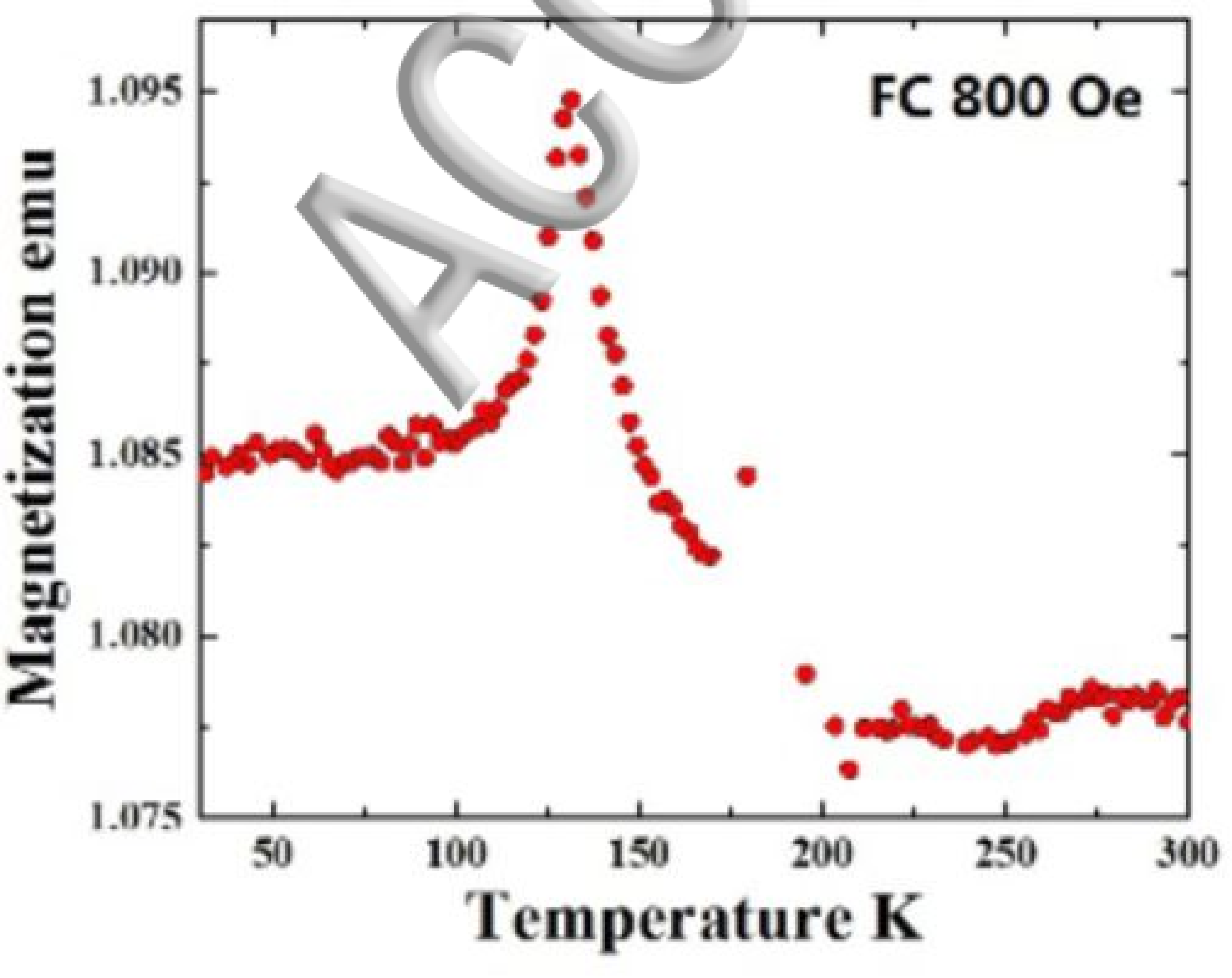
FC 800 Oe
Magnetization emu
1.095
1.090
1.085
1.080
1.075
50
100
150
200
250
300
Temperature K

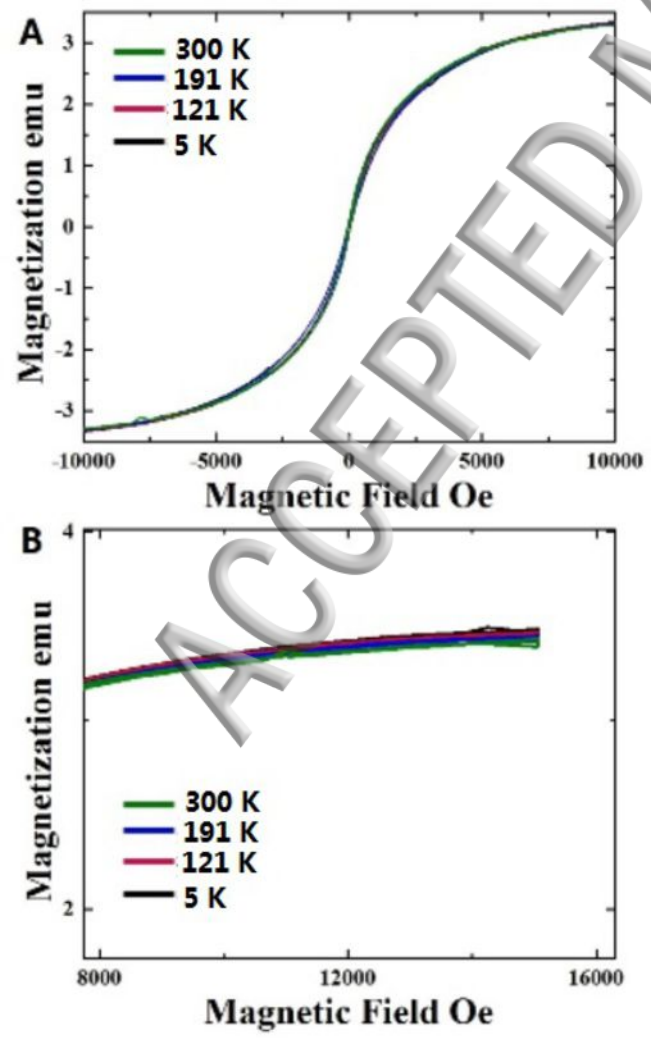
A
300 K
191 K
121 K
5 K
Magnetization emu
3
2
1
0
-1
-2
-3
-10000
-5000
0
5000
10000
Magnetic Field Oe
B
4
2
Magnetization emu
300 K
191 K
121 K
5 K
8000
12000
16000
Magnetic Field Oe

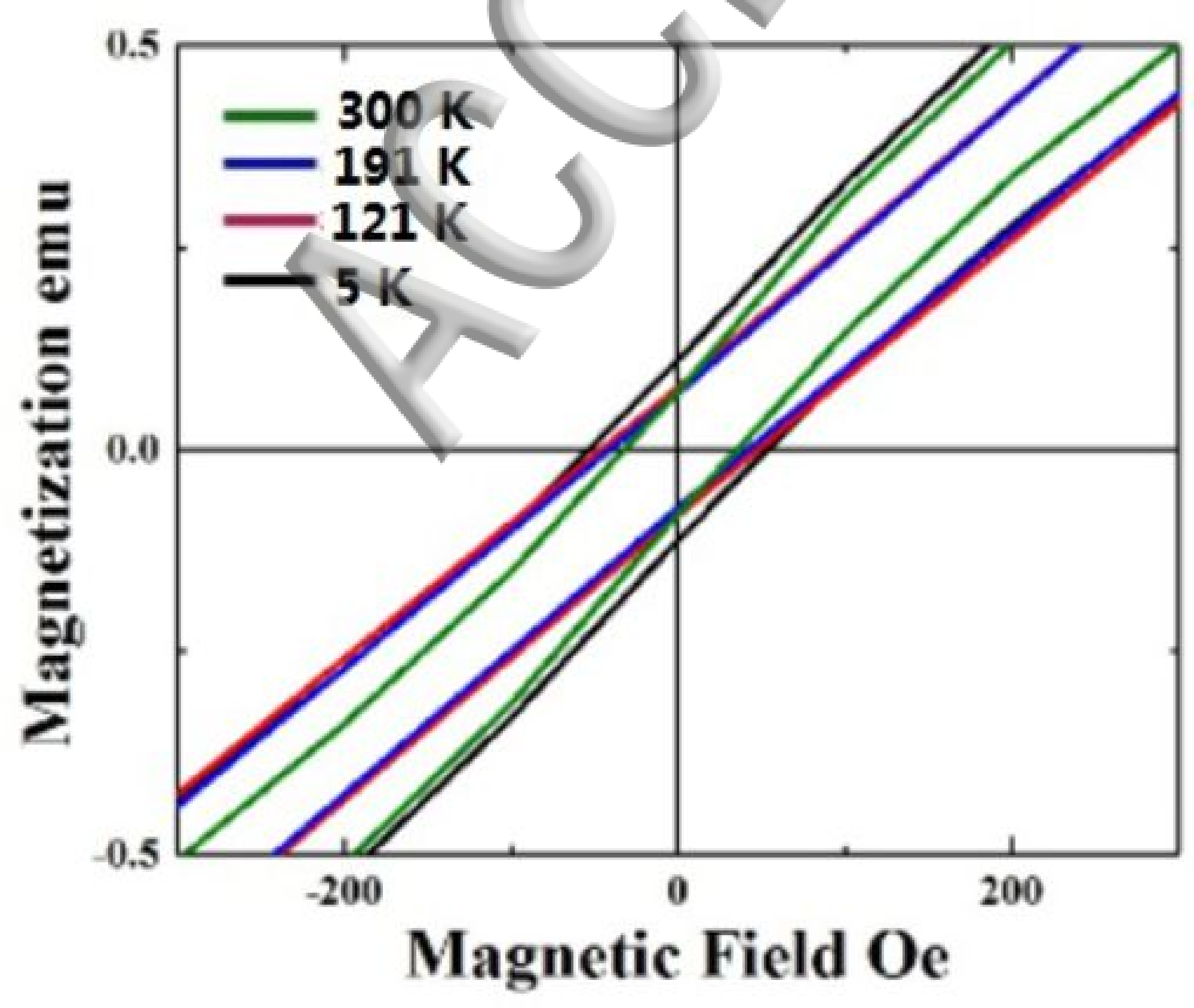
0.5
0.0
-0.5
-200
0
200
300 K
191 K
121 K
5 K
Magnetization emu
Magnetic Field Oe